

Salt-inducible kinases (SIKs) regulate TGF β -mediated transcriptional and apoptotic responses

Luke D. Hutchinson¹, Nicola J. Darling¹, Stephanos Nicolaou^{2,#}, Ilaria Gori², Daniel R. Squair¹, Philip Cohen¹, Caroline S. Hill² and Gopal P. Sapkota^{1*}

¹MRC Protein Phosphorylation and Ubiquitylation Unit, School of Life Sciences, University of Dundee, Sir James Black Centre, Dow Street, Dundee, DD1 5EH, United Kingdom.

²The Francis Crick Institute, 1 Midland Road, London, NW1 1AT, United Kingdom.

[#]Present address: The Institute of Cancer Research, 15 Cotswold Road, Sutton, London, SM2 5NG, United Kingdom.

*Correspondence and requests for materials should be addressed to: g.sapkota@dundee.ac.uk

Abstract

The signalling pathways initiated by members of the transforming growth factor- β (TGF β) family of cytokines control many metazoan cellular processes, including proliferation and differentiation, epithelial-mesenchymal transition (EMT), and apoptosis. TGF β signalling is therefore strictly regulated to ensure appropriate context-dependent physiological responses. In an attempt to identify novel regulatory components of the TGF β signalling pathway, we performed a pharmacological screen using a cell line engineered to report the endogenous transcription of the TGF β -responsive target gene *PAI-1*. The screen revealed that small-molecular inhibitors of salt-inducible kinases (SIKs) attenuate TGF β -mediated transcription of *PAI-1* without affecting receptor-mediated SMAD phosphorylation, SMAD complex formation or nuclear translocation. We provide evidence that genetic inactivation of SIK isoforms also attenuates TGF β -dependent transcriptional responses. Pharmacological inhibition of SIKs using multiple small-molecule inhibitors potentiated apoptotic cell death induced by TGF β stimulation. Our data therefore provides evidence for a novel function of SIKs in modulating TGF β -mediated transcriptional and cellular responses.

32

33 **Introduction**

34 Signalling pathways initiated by the TGF β family of cytokines are amongst the most
 35 prevalent and diverse in metazoan biology and regulate a multitude of processes including
 36 cellular proliferation and differentiation, epithelial-mesenchymal transition (EMT), cell
 37 migration, immunoregulation and apoptotic cell death in a context-dependent manner¹⁻⁶.
 38 Consequently, perturbations within the signalling pathway have been associated with the
 39 pathogenesis of many human disorders including cancer. For example, in normal epithelial
 40 cells, TGF β has a tumour suppressive function, principally through its ability to induce
 41 cytostasis and apoptotic cell death⁷⁻⁹. In contrast, during tumour progression, the
 42 suppressive effect of TGF β is lost and, in certain cancers, corruption of the signalling
 43 pathway can result in TGF β exerting a pro-oncogenic effect^{7,10,11}. Inhibition of the TGF β
 44 pathway has therefore been proposed as a potential therapeutic strategy in certain
 45 pathological contexts^{12,13}. However, the highly pleiotropic and context-dependent nature of
 46 TGF β signalling has provided a considerable challenge for pharmacological intervention¹⁴.
 47 Elucidating the context-dependent regulatory mechanisms underlying TGF β signalling is
 48 therefore of considerable importance in identifying novel therapeutic interventions.

49

50 TGF β signalling is initiated upon the binding of TGF β ligand dimers to cognate
 51 transmembrane receptor serine-threonine protein kinases to form activated
 52 heterotetrameric receptor complexes containing two type I receptors and two type II
 53 receptors¹⁵. This allows the constitutively active type II receptor to phosphorylate multiple
 54 serine and threonine residues within the cytoplasmic domain of the type I receptor, which
 55 enables the type I receptor to bind and phosphorylate the SMAD transcription factors 2/3
 56 (SMADs2/3) at the Ser-Xxx-Ser motif at the carboxy-terminal tail¹⁶⁻¹⁸. Receptor-mediated
 57 phosphorylation of R-SMADs facilitates interaction with the co-SMAD, SMAD4, followed by
 58 accumulation in the nucleus, where the SMAD complex co-operates with different
 59 transcriptional co-regulators to modulate the expression of hundreds of target genes in a
 60 cell type- and context-dependent manner¹⁸⁻²⁰.

61

Previously, we developed an endogenous transcriptional reporter cell line for the TGF β pathway using CRISPR-Cas9 genome editing technology²¹ by inserting firefly (*Photinus pyralis*) luciferase and green fluorescent protein (GFP) at the native TGF β -responsive target gene *plasminogen activator inhibitor 1 (PAI-1)* locus (Figure 1A). The transcription of *PAI-1* is induced in response to TGF β signals in different cell types in a SMAD-dependent manner^{22,23}. Moreover, the promoter region of the endogenous *PAI-1* gene has been frequently utilised in order to generate conventional luciferase-based overexpression reporter systems for the study of TGF β -mediated transcriptional regulation²⁴. In order to identify novel regulatory components of the TGF β pathway, we performed a pharmacological screen in this endogenous TGF β -responsive transcriptional reporter cell line using a panel of small-molecules obtained from the MRC International Centre for Kinase Profiling at the University of Dundee. The panel consisted predominantly of selective and potent inhibitors of protein kinases but also included a small number of compounds which target components of the ubiquitin-proteasome system (UPS). The screen identified salt-inducible kinases (SIKs), which are members of the AMPK-activated protein kinase (AMPK)-related subfamily of serine-threonine specific kinases^{25,26}, as potential novel regulators of TGF β -mediated gene transcription. In this study, we have therefore investigated the role of SIKs in regulating the TGF β signalling pathway.

Results

Identification of salt-inducible kinases (SIKs) as novel regulators of TGF β -mediated gene transcription

We tested the utility of the endogenous TGF β -responsive transcriptional reporter U2OS cell line (U2OS-2G) (Figure 1A) for a pharmacological screen. Stimulation of wild type (WT) U2OS and U2OS-2G cells with TGF β ₁ over 24 hours resulted in time-dependent induction of *PAI-1* and GFP expression respectively (Figure 1B), and comparable levels of SMAD3 C-terminal phosphorylation in both cell lines. TGF β induced a significant increase in relative luciferase activity in U2OS-2G cells over unstimulated cells, which was blocked with SB-505124, a selective inhibitor of the TGF β type I receptor (TGF β R1) kinases^{27,28} (Figure 1C). Similarly, TGF β -induced GFP expression in U2OS-2G cells is blocked with SB-505124 (Figure 1D). These data confirmed the suitability of U2OS-2G cells for pharmacological screens. A 96-well plate

format pharmacological screen was performed to identify potential novel regulators of the TGF β pathway (Figure 1E). TGF β R1 inhibitors SB-505124^{27,28} and A 83-01²⁹ served as positive controls, while DMSO a negative control. All compounds were used at 1 μ M final concentration. Both SB-505124 and A 83-01 significantly inhibited TGF β -induced luciferase activity compared with DMSO controls (Figure 1F and 1G). Additionally, D4476 and LDN193189, also significantly inhibited TGF β -induced luciferase activity. D4476 was initially identified as an inhibitor of TGF β R1³⁰, although subsequent *in vitro* profiling revealed that is inhibited casein kinase 1 (CK1) with greater potency³¹. LDN193189 is an ATP-competitive inhibitor of the BMP type I receptor kinases³². However, at 1 μ M concentration it also inhibits the TGF β R1²⁸. The majority of the compounds used in the screen did not significantly affect TGF β -induced luciferase reporter activity. Interestingly however, we observed that HG-9-91-01, a potent ATP-competitive inhibitor of salt-inducible kinase (SIK) isoforms³³, significantly attenuated TGF β -induced luciferase activity (Figure 1F and 1G), suggesting a possible role for SIKs in TGF β -induced transcription.

Characterisation of SIK inhibitors in the context of TGF β signalling

To explore the role of SIKs in TGF β signalling further, in addition to HG-9-91-01, we utilised MRT199665, a structurally distinct inhibitor of SIK isoforms³³ (Figure 2A). MRT199665 also suppressed TGF β -induced luciferase activity in U2OS-2G cells, as potently as SB-505124 and HG-9-91-01 (Figure 2B). Both HG-9-91-01 and MRT199665 inhibited the phosphorylation of a known SIK substrate CRTC3 at S370^{33–35} compared with DMSO control (Figure 2C). Because kinase inhibitors often display off-target inhibition, we tested whether the attenuation of TGF β -induced luciferase activity by HG-9-91-01 and MRT199665 occurred as a result of the off-target inhibition of the TGF β R1 upstream of SMAD2/SMAD3 phosphorylation. HG-9-91-01 substantially inhibited TGF β -induced SMAD3 phosphorylation, to a similar extent as SB-505124, compared to DMSO controls, whereas MRT199665 did not (Figure 2D), suggesting that HG-9-91-01 could inhibit either type I or type II TGF β receptors. Indeed, at concentrations of 0.1, 1 and 10 μ M *in vitro*, HG-9-91-01 inhibited TGF β R1 (ALK5) kinase activity, whereas MRT199664 did not (Figure 2E). Because of this off-target inhibition of TGF β R1 by HG-9-91-01, we decided to employ MRT199665 as SIK inhibitor for subsequent experiments.

MRT199665 attenuates the expression of endogenous TGF β target genes

Any compound that inhibits luciferase enzymatic activity could potentially yield a false-positive result in U2OS-2G cells. Therefore, to exclude this possibility for MRT199665, we tested whether the TGF β -induced GFP expression in U2OS-2G cells was affected by MRT199665. The TGF β -induced expression of GFP in U2OS-2G cells was inhibited with MRT199665, to the same extent as SB-505124, compared to DMSO control (Figure 3A), while the TGF β -induced SMAD2/SMAD3 C-terminal phosphorylation was unaffected by MRT199665 (Figure 3A). Moreover, MRT199665 significantly attenuated TGF β -induced *PAI-1* mRNA expression in WT U2OS cells (Figure 3B). In WT A-172 human glioblastoma cells, MRT199665 also inhibited TGF β -induced expression of *PAI-1* mRNA, as well *SMAD7* and connective tissue growth factor (*CTGF*) mRNAs (Figure 3C). These data demonstrate that MRT199665 inhibits TGF β -induced transcription of endogenous target genes in different cells without affecting SMAD2/SMAD3 phosphorylation.

Genetic inactivation of SIK2/3 attenuates the TGF β -mediated induction of PAI-1 expression

We employed genetic approaches to test the impact of SIK kinase activity on TGF β signalling. SIKs are members of the AMP-activated protein kinase (AMPK)-related subfamily of serine-threonine protein kinases that require LKB1-mediated phosphorylation of a conserved threonine residue within the activation loop in order to become catalytically active^{25,26} (Figure 4A). In LKB1-deficient WT HeLa cells^{36–38}, TGF β_1 induced a 1.5-fold increase in *PAI-1* mRNA expression relative to unstimulated controls. However, stable overexpression of catalytically active LKB1 (LKB1^{WT}), but not catalytically inactive mutant (LKB1^{D194A}), in WT HeLa cells significantly enhanced the TGF β -induced transcription of *PAI-1* mRNA (Figure 4B) as well as PAI-1 protein levels (Figure 4C), although the levels of LKB1^{WT} restored in HeLa cells was substantially higher than the LKB1^{D194A} mutant (Figure 4C).

The catalytic activity of SIK isoforms can be ablated via mutation of the activation loop threonine to alanine³⁹, which abolishes LKB1-mediated phosphorylation. Indeed, in mouse embryonic fibroblasts (MEFs) derived from embryos harbouring homozygous SIK2^{T175A} and

SIK3^{T163A} genotypes³⁹, the phosphorylation of CRTC3 at S370 is substantially reduced compared to WT control MEFs (Figure 4D). A time-course treatment WT MEFs with TGFβ₁ resulted in robust SMAD3 phosphorylation and increase in PAI-1 protein levels at 6 hours (Figure 4E). When homozygous SIK2^{T175A}/SIK3^{T163A} MEFs were subjected to TGFβ stimulation for 6 hours, the induction of PAI-1 protein expression was substantially attenuated compared with WT MEFs, despite the observation of higher SMAD3 phosphorylation in the SIK2^{T175A}/SIK3^{T163A} mutant MEFs (Figure 4F). Consistent with this, the relative *PAI-1* mRNA expression in response to TGFβ stimulation was significantly reduced in MEFs derived from two independent homozygous SIK2^{T175A}/SIK3^{T163A} mice relative to WT MEFs (Figure 4G).

Impact of SIK isoforms on TGFβ-dependent proliferative responses

TGFβ inhibits epithelial cell proliferation, in part through transcriptional upregulation of cyclin-dependent kinase (CDK) inhibitors p21^{CIP1} and p27^{KIP1} and downregulation of the proto-oncogene c-Myc^{1,4,7}. In HaCaT cells, we observed an increase in endogenous p27^{KIP1} and p21^{CIP1} protein levels and a decrease in c-Myc protein levels over a 24-hour time course of TGFβ treatment (Figure 5A). Rather surprisingly, treatment of HaCaT cells with MRT199665 resulted in increased expression of both p21^{CIP1} and p27^{KIP1} even in the absence of TGFβ treatment, and this increase was more pronounced after stimulation of cells with TGFβ compared to DMSO controls (Figure 5B). This suggested that inhibition of SIKs alone may exert cytostatic effects. When we analysed the proliferation of HaCaT cells over a period of 160 hours, the control cells displayed a typical sigmoid growth curve, while TGFβ treatment caused a significant inhibition of proliferation after 100 hours (Figure 5C). Under these conditions, MRT199665 profoundly suppressed cell proliferation at all time points, regardless of TGFβ treatment (Figure 5C). We also observed a substantial increase in p27^{KIP1} levels in MEFs derived from homozygous SIK2^{T175A}/SIK3^{T163A} KI mice relative to WT mice irrespective of TGFβ stimulation (Figure 5D), suggesting that SIK kinase activity plays a fundamental role in suppressing p27^{KIP1} protein levels. To further confirm that SIK inhibition promotes cytostasis independent of TGFβ stimulation, we exploited SMAD3^{-/-} HaCaT cells and showed that treatment of both WT and SMAD3^{-/-} HaCaT cells with MRT199665 resulted in an increase in p21^{CIP1} and p27^{KIP1} levels compared with untreated control cells (Figure 5E).

In many epithelial cells TGF β -induced cytostasis, through the induction of p21^{CIP1} and p27^{KIP1} and suppression of c-Myc, is often necessary for subsequent TGF β -dependent cell fates, such as differentiation, epithelial-mesenchymal transition (EMT) and apoptosis. Our unexpected findings that inhibition of SIK isoforms induces the expression of p21^{CIP1} and p27^{KIP1} levels independent of TGF β prompted us to explore whether TGF β -induced epithelial cell fates are sensitised by SIK inhibitors. We therefore sought to investigate whether inhibition of SIK isoforms sensitises cells to TGF β -induced EMT and apoptosis.

Pharmacological inhibition of SIKs potentiates TGF β -mediated apoptosis

NMuMG murine mammary epithelial cells undergo both EMT and apoptosis upon TGF β stimulation^{40–44}. When we tested the effect of MRT199665 on TGF β -induced EMT in NMuMG cells, which usually takes around 24-48 hours, it became apparent that there was profound cell death within 12-24 hours, prompting us to investigate apoptosis. The apoptotic response to TGF β is mediated in part by the executioner cysteine-aspartic acid protease, caspase-3. Caspase-3 is synthesised as an inactive proenzyme and requires proteolytic cleavage in order to become catalytically active. Apoptosis can thus be monitored via the detection of the cleaved, and hence activated, form of caspase-3. Furthermore, activated caspase-3 mediates the proteolytic cleavage of poly (ADP-ribose) polymerase (PARP), which can also be used to monitor apoptosis. Stimulation of NMuMG cells with TGF β ₁ over a period of 72 hours induced the activation of caspase-3 and subsequent cleavage of PARP, with maximal cleavage observed at 24 hours (Figure 6A). The expression of pro-apoptotic factor Bim was observed at 48-72 hours (Figure 6A). In these cells, SIK inhibitors HG-9-91-01 and MRT199665 resulted in reduction of phospho-CRTC3-S370 (Figure 6B). The TGF β -induced cleavage of caspase-3 and PARP at 24 hours was blocked by SB-505124 (Figure 6C). Interestingly, in cells incubated with MRT199665 and TGF β ₁, the appearance of cleaved caspase-3 and PARP were substantially enhanced compared with TGF β -treated DMSO controls (Figure 6C). In the absence of TGF β ₁, MRT199665 alone did not induce the cleavage of caspase-3 and PARP (Figure 6D). Furthermore, MRT199665+TGF β ₁ treatment resulted in the maximal and more pronounced appearance of cleaved caspase-3 and PARP much earlier (12 hours) than TGF β ₁ alone treatment (Figure 6D). When we monitored apoptosis using Annexin V and DAPI staining, treatment of NMuMG cells with TGF β for 24 hours resulted in a substantial increase in

Annexin V-positive apoptotic cells over controls, while this was reversed by SB-505124. Treatment of cells with MRT199665 significantly enhanced TGF β -induced apoptosis (Figure 6E). Similarly, when we analysed cell viability, TGF β ₁ treatment resulted in a decrease in the number of viable cells compared with DMSO control, while this was reversed by the SB-505124 (Figure 6F). In contrast, treatment of cells with MRT199665 resulted in almost complete loss of viable cells (Figure 6F). Collectively, these results indicate that inhibition of SIK isoforms by MRT199665 can potentiate TGF β -mediated apoptotic cell death in NMuMG cells.

Previous reports have revealed that the clinically approved tyrosine kinase inhibitors (TKIs) bosutinib and dasatinib are also capable of inhibiting SIK isoforms, with *in vitro* IC₅₀ values in the low nanomolar range^{45,46} (Figure 7A). Both bosutinib and dasatinib inhibit the kinase activity of the BCR-Abl fusion as well as Src and BTK (Figure 7B) and are used to treat Philadelphia chromosome positive (Ph+) chronic myelogenous leukaemia (CML) and acute lymphoblastic leukaemia (ALL)^{47,48}. In WT U2OS cells, both compounds reduced the phospho-CRTC3 (S370) levels compared to DMSO controls, suggesting effective SIK inhibition (Figure 7C). Like MRT199665, neither bosutinib nor dasatinib inhibited the TGF β -induced phosphorylation of SMAD2/SMAD3 but both inhibited the TGF β -induced expression of GFP in U2OS 2G cells (Figure 7D), and endogenous PAI-1 in WT U2OS cells (Figure 7E). As in U2OS cells, in NMuMG cells, neither compound affected the TGF β -induced phosphorylation of SMAD2/3 relative to controls (Figure 7F). Excitingly, treatment of NMuMG cells with bosutinib for 24 hours substantially enhanced the TGF β -induced levels of cleaved caspase-3 and PARP to a similar extent as MRT199665 (Figure 7G), suggesting that the increased TGF β -induced apoptosis caused by bosutinib is likely due to its ability to inhibit SIK isoforms.

SIKs do not appear to affect SMAD2/3 phosphorylation and their nuclear translocation directly

We sought to investigate the molecular mechanisms by which SIK2/SIK3 might regulate TGF β signalling. To explore whether SIKs exert effects on TGF β signalling through direct phosphorylation of SMAD proteins, *in vitro* kinase assays were performed. GST-SIK2 and GST-SIK3, but not MBP-SIK1, phosphorylated SMAD2, SMAD3 and SMAD4 *in vitro* (Figure

S1), while SIK inhibitor HG-9-91-01 blocked SMAD3 phosphorylation (Figure S2). Mass spectrometry identified Thr247 as the predominant SIK2/3 phosphorylated residue on SMAD3. This residue is conserved in SMAD2, SMAD3, SMAD4 and SMAD9 proteins (Figure 8A). The TGF β -induced transcription of *PAI-1* has been previously reported to be specific to SMAD3^{23,49}. Consistent with this, treatment of wild type and SMAD3^{-/-} HaCaT cells with human TGF β ₁ resulted in C-terminal phosphorylation of SMAD2 however PAI-1 expression was completely abrogated in SMAD3^{-/-} cells but not in WT cells (Figure 8B). Transient restoration of SMAD3 expression with FLAG-SMAD3^{WT} was sufficient to partially restore TGF β -induced PAI-1 expression (Figure 8D). However, restoration of the SIK-phospho-deficient mutant FLAG-SMAD3^{T247A} in SMAD3^{-/-} cells also restored TGF β -induced PAI-1 expression, to similar levels observed with SMAD3^{WT} (Figure 8B), suggesting that phosphorylation of SMAD3 at Thr247 by SIKs is unlikely to explain effects of SIKs in TGF β signalling.

Next, we whether SIK2/SIK3 inhibition disrupts the formation of SMAD2/SMAD3-SMAD4 complexes or nuclear accumulation of SMADs. In U2OS cells stably overexpressing GFP-SMAD4, neither the basal nor TGF β -induced increase in co-precipitation of SMAD2/3 in GFP-SMAD4 IPs was affected by treatment of cells with MRT199665 (Figure 8C). TGF β -induced a robust nuclear accumulation of phosphorylated SMAD2 and SMAD3 levels in nuclear fractions over unstimulated conditions or when cells were treated with SB-505124 (Figure 8D). MRT199665 treatment did not affect the cytoplasmic/nuclear distribution of phosphorylated SMAD2/SMAD3 relative to controls in both unstimulated and TGF β ₁ stimulated conditions (Figure 8D). Consistent with this, in cells stably overexpressing GFP-SMAD2, MRT199665 did not prevent the nuclear translocation of GFP-SMAD2 following TGF β ₁ stimulation when analysed via immunofluorescence (IF) (Figure 8E). As inhibition of SIK isoforms with MRT199665 does not appear to impact the formation of the SMAD2/3-SMAD4 complex or the nuclear accumulation of phosphorylated SMAD2/3, the effect of MRT199665 is likely to occur further downstream.

Discussion

In this study, we identified inhibitors of SIK isoforms as novel candidates for the inhibition of TGF β -induced transcription. We established that inhibiting SIK protein kinase activity, both pharmacologically and genetically, attenuates the TGF β -induced expression of endogenous *PAI-1* transcript and protein in different cells. Moreover, the attenuation of TGF β -induced *PAI-1* by MRT199665 occurred without affecting phosphorylation of SMAD proteins, the SMAD2/SMAD3-SMAD4 interaction or the nuclear accumulation of activated SMADs. We propose that SIK isoforms function at the level of transcriptional regulation in the context of TGF β signalling.

In every cell line we tested, TGF β -induced endogenous *PAI-1* transcript and protein levels were reduced by both pharmacological and genetic ablation of SIK kinase activity. *PAI-1* is a serine protease inhibitor (Serpin) that functions as the physiological inhibitor of the serine proteases tissue-type plasminogen activator (t-PA) and urokinase-type plasminogen activator (u-PA) and controls fibrinolysis. Increased plasma levels of *PAI-1* have been associated with a number of diseases including thrombotic vascular disorders⁵⁰. As inhibition of SIK isoforms attenuates TGF β -induced expression of *PAI-1*, pharmacological SIK inhibitors may have novel therapeutic potential if they demonstrably suppress excessive *PAI-1* levels *in vivo*.

SIK1 was previously linked to the regulation of TGF β signalling^{51,52} in which it was shown that SIK1 was a direct transcriptional target of TGF β signalling and played a role in the degradation of ALK5 through SIK1/SMAD7/SMURF2 complex. During the course of our experiments, we did not observe any change in protein of expression of either SIK2 or SIK3 upon TGF β signalling, suggesting that unlike SIK1, these two isoforms are not transcriptional targets of TGF β signalling. Our data indicates that the inhibition of the kinase activity of SIK2 and SIK3 is sufficient to suppress the TGF β -induced upregulation of *PAI-1*, whereas RNAi-mediated depletion of SIK1 has been reported to enhance *PAI-1* mRNA expression in response to TGF β stimulation⁵¹. It is therefore apparent that the exact roles of the different SIK isoforms in regulating TGF β signalling remains to be elucidated and is most likely context dependent.

The precise mechanisms by which SIK isoforms regulate the TGF β -induced expression of *PAI-1* or other genes remains to be resolved. As serine-threonine protein kinases, SIK isoforms act by phosphorylating protein substrates. In the case of TGF β signalling, these could be components of the SMAD-transcriptional complexes or key transcriptional modulators, enhancers, suppressors as and/or adaptors that modulate the function of these transcriptional co-factors in order to control the transcriptional activity of SMAD2/SMAD3. Unless the core SMAD2/3 transcriptional complexes are found to be substrates of SIKs, the impact of SIKs in TGF β -target gene transcription is likely to be determined by whether the individual target gene promoters recruit specific SIK substrates. It is known that SMAD2/SMAD3 do not directly regulate target gene transcription, but instead facilitate the recruitment of various transcriptional co-activators/co-repressors or histone modifying enzymes²⁰. SIKs have been reported to regulate the Toll-like Receptor (TLR) signalling through their ability to phosphorylate the transcriptional coactivator CRTC3 and so reduce CREB-dependent transcription of the *IL10* gene³³. It is therefore conceivable that SIKs may employ similar mechanisms to regulate SMAD-associated transcriptional co-factors to modulate the transcription of specific subsets of TGF β -target genes. A phospho-proteomic approach using both SIK inhibitors and SIK2^{T175A}/SIK3^{T163A} MEFs might uncover potential SIK substrates that underpin the regulation of TGF β -induced transcription of distinct genes.

In many epithelial cell types, TGF β -induced cytostasis through p15^{INK4B}, p21^{CIP1} and p27^{KIP1} 1,4 is often followed by context-dependent cell fates, such as differentiation, epithelial-mesenchymal transition (EMT) or apoptosis^{53,54}. Interestingly, inhibition of SIKs induced p21^{CIP1} and p27^{KIP1} expression independently of TGF β stimulation. Perhaps due in part to this, SIK inhibitors sensitise NMuMG cells for TGF β -induced apoptosis. These observations imply that SIK inhibitors could be employed to sensitise cancer cells for apoptosis in those cells that TGF β induces apoptosis. This could be easily tested by using clinically approved anti-cancer drugs dasatinib and bosutinib that inhibit SIK isoforms in addition to their intended targets in a number of cancer cell types, including multiple Burkitt's lymphoma (BL) cell lines^{42,55-57}, hepatocellular carcinoma⁵⁸ and prostate carcinoma cells⁵⁹⁻⁶¹ that have been reported to undergo apoptosis in response to TGF β .

Our findings place SIK isoforms as modulators of a subset of TGF β -induced transcriptional and physiological responses. Understanding these in detail will allow targeting of selective TGF β responses, thereby limiting potential consequences of inhibiting the TGF β pathway in its entirety. Of course, as discussed above, SIKs themselves are known to control other pathways, including immune signalling, and these need to be considered carefully. Taking into consideration that the clinically approved TKIs dasatinib and bosutinib, which also potentially inhibit SIK isoforms^{45,46}, are administered to patients safely, it is conceivable that more specific SIK inhibitors could be applied to target certain TGF β -associated pathologies.

Materials and methods

Antibodies

For Western immunoblotting analysis, all primary IgG antibodies were used at 1:1000 dilution unless otherwise stated. Anti-Phospho-SMAD3 (S423/S425) Rabbit polyclonal IgG (600-401-919) was purchased from Rockland Inc. Anti-GFP Mouse monoclonal IgG (11814460001) was purchased from Roche. Anti-Phospho-SMAD2 (S465/S467) Rabbit polyclonal IgG (3101), anti-SMAD2/3 Rabbit monoclonal IgG (8685), anti-c-Myc Rabbit monoclonal IgG (5605), anti-p27^{KIP1} Rabbit monoclonal IgG (3688), anti-p21^{WAF1/CIP1} Rabbit monoclonal IgG (2947), anti-GAPDH Rabbit monoclonal IgG (used at 1:5000 dilution) (2118), anti-SIK2 Rabbit IgG (6919) were all purchased from Cell Signalling Technology (CST). Anti-PAI-1 Rabbit polyclonal IgG (ab66705), anti-CTGF Rabbit polyclonal IgG (ab6992) and anti-CRTC3 Rabbit monoclonal IgG (ab91654) were purchased from Abcam. Anti-Phospho-CRTC3 (S370) Sheep polyclonal IgG (S253D, 3rd bleed) and anti-SIK3 Sheep polyclonal IgG (S373D, 3rd bleed) were generated by MRC PPU Reagents and Services. Species-specific horseradish peroxidase (HRP)-conjugated secondary antibodies were used at 1:2500-5000 dilution. Rabbit anti-Sheep polyclonal IgG (H+L) Secondary Antibody, HRP (31480) and Goat anti-Mouse polyclonal IgG (H+L) Secondary Antibody, HRP (31430) were purchased from Thermo Fisher Scientific. Goat anti-Rabbit polyclonal IgG (H+L), HRP-conjugated Secondary Antibody (7074) was purchased from CST.

Cytokines and pharmacological inhibitors

Purified recombinant human TGF β ₁ was purchased from either R&D Systems or PeproTech and reconstituted in sterile 4 mM HCl containing 1 mg mL⁻¹ bovine serum albumin (BSA). Prior to stimulation with TGF β ₁, cells were cultured in serum-free culture media for approximately 16 hours at 37°C in order to reduce autocrine signalling. Pharmacological inhibitors were reconstituted at 10 mM in dimethyl sulfoxide (DMSO) and used at the concentrations and durations indicated in the respective figure/figure legend. For all inhibitor experiments, control cells were incubated with an equivalent volume of DMSO.

Generation of SIK KI mice

SIK2^{T175A}/SIK3^{T163A} homozygous kinase dead knock-in (KI) mice were bred from SIK2^{tm1.1Arte} and SIK3^{tm1.1Arte} mice maintained on a C57BL/6NJ genetic background as described previously³⁹. Primary mouse embryonic fibroblasts (MEFs) were generated from SIK2^{T175A}/SIK3^{T163A} or SIK3^{WT} embryos at E11.5-13.5 as detailed previously⁶². Primary and SV-40 immortalised MEFs were cultured in DMEM supplemented with 20% (v/v) FBS, 2 mM L-glutamine, 100 units mL⁻¹ Penicillin, 100 µg mL⁻¹ Streptomycin, 1x Minimum Essential Medium (MEM) Non-Essential Amino Acids (NEAA) and 1 mM Sodium Pyruvate. Mice were maintained in individually ventilated cages and provided with free access to food and water under specific pathogen-free conditions consistent with E.U. and U.K. regulations. All animal breeding and studies were conducted following approval by the University of Dundee Ethical Review Committee and performed under a U.K. Home Office Project Licence granted under the Animals (Scientific Procedures) Act 1986.

Mammalian cell culture

A-172 human glioblastoma, A549 human pulmonary adenocarcinoma, U2OS human osteosarcoma, HACAT human immortalised keratinocyte, HEK-293 human embryonic kidney and HeLa human cervical adenocarcinoma cells were obtained from the MRC PPU Tissue Culture facility and cultured in Dulbecco's Modified Eagle's Medium (DMEM) supplemented with 10% (v/v) fetal bovine serum (FBS), 2 mM L-glutamine, 100 units mL⁻¹ Penicillin and 100 µg mL⁻¹ Streptomycin (hereafter referred to as D10F media). NMuMG murine mammary epithelial cells were cultured in D10F media supplemented with 10 µg mL⁻¹ insulin (from

bovine pancreas). All cell lines were maintained at 37°C in a humidified atmosphere with 5% (v/v) CO₂ levels and routinely tested for mycoplasma contamination.

Generation of *SMAD3*^{-/-} knockout cells using CRISPR-Cas9

To generate *SMAD3*^{-/-} knockout cells by CRISPR-Cas9 genome editing, HaCaT cells were transfected with the plasmid pSpCas9(BB)-2A-GFP (PX458)⁶³ containing both the Cas9 endonuclease and a guide RNA (gRNA) pair targeting exon 6 of the endogenous *SMAD3* gene. For the acquisition of single-cell knockout clones, single cells were isolated by fluorescence-activated cell sorting (FACS) and plated in individual wells of 96-well cell culture plates. Viable cell clones were expanded, and successful knockouts confirmed by both Western immunoblotting and genomic DNA sequencing. Sequence of gRNA oligonucleotides: *SMAD3* forward gRNA 5'-CACCGGAATGTCTCCCCGACGCGC-3'; *SMAD3* reverse gRNA 5'-AAACGCGCGTCGGGGAGACATTCC-3'.

Mammalian cell lysis

Cells were washed twice with cold 1x DPBS and incubated with lysis buffer (50 mM Tris/HCl pH 7.5, 270 mM sucrose, 150 mM sodium chloride, 1 mM EDTA pH 8.0, 1 mM EGTA pH 8.0, 1 mM sodium orthovanadate, 10 mM sodium β-glycerophosphate, 50 mM sodium fluoride, 5 mM sodium pyrophosphate, 1% (v/v) Nonidet P-40 (NP-40)) supplemented with Complete, EDTA-free Protease Inhibitors (Roche) (one tablet per 25 mL) for approximately 5 minutes on ice. Cell lysates were transferred to 1.5 mL microcentrifuge tubes and centrifuged at 16,000 x g for 10 minutes at 4°C and either processed immediately or cryopreserved in liquid nitrogen prior to storage at -80°C. The protein concentrations of the cell lysate samples were determined using Pierce Coomassie (Bradford) Protein Assay Kit (Thermo Fisher Scientific). Cell lysate samples were subsequently diluted using 4x NuPAGE LDS (lithium dodecyl sulfate) sample buffer (Invitrogen) supplemented with 8% (v/v) 2-Mercaptoethanol (2-ME) (Sigma-Aldrich) and the sample concentrations equalised.

Luciferase transcriptional reporter assay

U2OS 2G transcriptional reporter cells were seeded in 6-well cell culture plates and incubated with the required small-molecule inhibitors/cytokine at the indicated

concentrations and duration. Cells were subsequently washed twice with 1x DPBS and lysed using 1x Cell Culture Lysis Reagent (CCLR; Promega). Cell culture plates were incubated for approximately 5 minutes on bench-top platform rocker to ensure efficient cell lysis. Cell lysates were transferred to 1.5 mL microcentrifuge tubes and kept on ice. Lysate samples were vortexed for approximately 10 seconds, centrifuged at 12,000 x g for 2 minutes at 4°C and 200 µL of supernatant transferred to new 1.5 mL microcentrifuge tubes. Lysate samples were subsequently transferred to 96-well white flat-bottom cell culture microplates. An equivalent volume of 2x Luciferase Assay Buffer (50 mM Tris/Phosphate pH 7.8, 16 mM MgCl₂, 2 mM dithiothreitol (DTT), 1 mM adenosine triphosphate (ATP), 30% (w/v) glycerol, 1% (w/v) bovine serum albumin (BSA), 250 µM *D*-Luciferin, 8 µM sodium pyrophosphate) was subsequently added to each well and the microplate incubated for approximately 1 minute on a bench-top vibrating platform. Luminescence values were obtained using an EnVision 2104 Multimode Microplate Reader (PerkinElmer). The protein concentrations of each lysate sample were determined using Pierce Coomassie (Bradford) Protein Assay Kit (Thermo Fisher Scientific) and used to normalise luminescence values.

Cellular fractionation

Extraction of separate cytoplasmic and nuclear protein fractions from cultured U2OS cells was performed using NE-PER Nuclear and Cytoplasmic Extraction Reagents (Thermo Fisher Scientific) according to the manufacturer's protocol. The supplied lysis buffers (CER I and NER) were supplemented with 1x Complete, EDTA-free Protease Inhibitors (Roche) immediately prior to use. Subcellular fractions were reduced using NuPAGE 4x LDS sample buffer containing 8% (v/v) 2-mercaptoethanol and incubated at 95°C for 5 minutes prior to SDS-PAGE. Fractions were resolved by SDS-PAGE and analysed via Western immunoblotting.

Quantitative reverse transcription polymerase chain reaction (RT-qPCR)

For all RT-qPCR experiments, cells were seeded in 6-well cell culture plates and incubated with the required TGFβ₁/inhibitor combinations for the durations indicated in the respective figure legends. Total RNA was isolated from the cells using the RNeasy Micro Kit (Qiagen) according to the manufacturer's protocol. Complementary DNA (cDNA) was synthesised from 0.5-1.0 µg of isolated RNA using iScript cDNA Synthesis Kit (Bio-Rad) according to the manufacturer's protocol. All RT-qPCR reactions were conducted in triplicate and included

50% (v/v) SsoFast EvaGreen Supermix (Bio-Rad), 0.5 μ M forward primer, 0.5 μ M reverse primer and the required volume of cDNA. RT-qPCR experiments were performed using CFX96 or CFX384 Real-Time PCR Detection Systems (Bio-Rad). The Ct (cycle threshold) values for each gene of interest were normalised to the arithmetic mean Ct value of the reference gene glyceraldehyde-3-phosphate dehydrogenase (GAPDH) or 18S ribosomal RNA (rRNA) using Microsoft Excel software. The $2^{-\Delta\Delta Ct}$ relative quantification method was then used to analyse the relative changes in gene expression between control and treatment conditions⁶⁴. GraphPad Prism software (version 8.0) was used to generate graphs and perform statistical analysis.

Immunofluorescence (IF) microscopy

U2OS GFP-SMAD2 cells were plated onto glass coverslips and treated as described in the respective figure legends. Cells were fixed in 4% (w/v) paraformaldehyde (PFA) immediately after aspirating culture media for 15 minutes at RT before washing twice in 1x PBS. Permeabilisation was performed using 0.2% Triton X (Sigma) in PBS for 10 minutes at RT before washing twice more in 1x PBS and blocking for 1 hour at RT with 5% (w/v) BSA in PBS. Primary antibody (anti-GFP polyclonal IgG, 1:1000 dilution) in 0.5% BSA/0.2% TWEEN 20 (Sigma)/PBS was added to coverslips for 1 hour at 37°C before washing three times in 0.5% BSA/0.2% TWEEN 20/PBS (10 minutes per wash). Cells were incubated with the secondary Alexa-Fluor conjugated antibody (anti-Rabbit, 488 nm; 1:500 dilution) for 1 hour at RT, before washing with 0.5% BSA/0.2% TWEEN 20 /PBS three times (20 minutes per wash). During the second wash of the three, 4',6-Diamidino-2-Phenylindole Dihydrochloride (DAPI; Sigma) was added at a final concentration of 1 μ g mL⁻¹ and removed in the final wash. Coverslips were rinsed in deionised H₂O and mounted onto glass microscopy slides using VECTASHIELD (Vector Laboratories). Coverslips were sealed and left to dry overnight at 4°C. Cells were imaged using the DeltaVision Imaging System (20x or 60x objective; GE Healthcare) and processed using softWoRx (GE Healthcare) and OMERO⁶⁵.

Annexin V staining assay

NMuMG cells were incubated with the required cytokine/inhibitor combinations. Following this, both adherent and non-adherent (*i.e.* apoptotic) cells were collected into 50 mL conical centrifuge tubes, pelleted by centrifugation (300 x g, 2 minutes) and washed once using cold

1x DPBS. Cells were subsequently centrifuged (300 x g, 2 minutes), the cell pellets were resuspended in Annexin Binding Buffer, ABB (10 mM HEPES, 140 mM NaCl, 2.5 mM CaCl₂, pH 7.4) and transferred to 1.5 mL microcentrifuge tubes. The required cell suspension samples were then incubated with Annexin V, Alexa Fluor 488 conjugate (Invitrogen; A13201) for 15 minutes at RT and protected from light. The appropriate samples were subsequently incubated with 5 µg mL⁻¹ DAPI (4',6-diamidino-2-phenylindole) (Invitrogen). Samples were immediately analysed using a BD LSRFortessa Cell Analyser (BD Biosciences) and BD FACSDiva acquisition software (BD Biosciences). Annexin V Alexa Fluor 488 fluorescence was detected by excitation at 488 nm and emission at 530 ± 30 nm, and DAPI fluorescence was detected by excitation at 355 nm and emission at 450 ± 50 nm. Single cells were identified on the basis of forward light scatter (FSC) and side light scatter (SSC), and subsequently evaluated for Annexin V Alexa Fluor 488 and DAPI fluorescence. Data analysis was performed using FlowJo Single Cell Analysis Software (BD Biosciences).

Cellular proliferation

HaCaT cells were assayed for proliferation using an IncuCyte ZOOM Live-Cell Analysis System (Sartorius). Cells were plated in 96-well cell culture plates (1 x 10³ cells per well, 6 wells per condition, plates in triplicate) and incubated with the required small-molecule inhibitor in the presence or absence of recombinant human TGFβ₁ (5 ng mL⁻¹). Cells were imaged every 2 hours over a period of 170 hours and the percent confluence determined using IncuCyte ZOOM Analysis Software (Sartorius).

Crystal violet cellular viability assay

NMuMG cells were seeded in 96-well cell culture plates and incubated for 24 hours at 37°C to enable adherence of cells to culture plates. The inclusion of wells containing culture medium without cells were used as negative control wells. Following initial 24-hour incubation, culture media was aspirated and replaced with reduced serum (1% v/v FBS) DMEM supplemented with 10 µg mL⁻¹ bovine insulin (Sigma-Aldrich) containing the required inhibitors or equivalent volume DMSO, with or without recombinant human TGFβ₁ (5 ng mL⁻¹) and incubated for a further 24 hours. Cells were subsequently fixed using 10% (v/v) methanol/10% (v/v) acetic acid for 5 minutes at RT and subsequently washed with 1x PBS. Fixed cells were stained using 0.5% (w/v) crystal violet staining solution (0.5 g crystal violet

powder (Sigma-Aldrich), 80 mL distilled H₂O and 20 mL methanol) for 20 minutes at RT on a bench-top platform rocker. Plates were subsequently washed carefully using tap water, inverted on filter paper to remove residual liquid and allowed to air-dry overnight. Following this, methanol was added to each well and incubated for 20 minutes at RT on a bench-top platform rocker. The absorbance value of each well was measured at 570 nm (OD₅₇₀) using a 96-well microplate spectrophotometer. The mean OD₅₇₀ value of negative control wells (*i.e.* wells not containing cells) was subtracted from the values obtained from each well on the culture plate and the percentage of viable cells for each condition determined relative to the mean average OD₅₇₀ value of non-stimulated DMSO control treated cells.

***In vitro* protein kinase assay**

21 µL reaction solutions were prepared containing 200 ng of protein kinase and 2 µg of substrate protein in 1x kinase assay buffer (50 mM Tris-HCl pH 7.5, 0.1 mM EGTA, 10 mM magnesium acetate, 0.1% (v/v) 2-mercaptoethanol and 0.1 mM [γ ³²P]-ATP). Reactions were conducted at 30°C for 30 minutes at 1050 rpm and terminated via the addition of 7 µL NuPAGE 4x LDS sample buffer containing 8% (v/v) 2-mercaptoethanol. For *in vitro* kinase assays involving the use of small-molecule inhibitors, reaction solutions containing all the required components were incubated at 30°C for 10 minutes at 1050 rpm prior to the addition of 0.1 mM [γ 32P]-ATP. Reactions were then performed as detailed previously. Samples were incubated at 95°C for 5 minutes and subsequently centrifuged at 5.0 x 10³ x g for 1 minute. Samples were loaded onto NuPAGE 4-12% Bis-Tris precast polyacrylamide gels and resolved via SDS-PAGE. Polyacrylamide gels were subsequently stained with InstantBlue Coomassie Protein Stain (Expedeon) to visualise the resolved recombinant proteins and imaged using the ChemiDoc Imaging System (Bio-Rad). ³²P radioactivity was analysed via autoradiography using Amersham Hyperfilm (GE Healthcare Life Sciences).

Statistical analysis

All experiments have a minimum of three biological replicates unless otherwise stated in the respective figure legend. In addition, all luciferase, RT-qPCR, cellular proliferation, annexin V staining and crystal violet staining experiments have at least three technical repeats for each biological replicate. The data are presented as the arithmetic mean with error bars

denoting the standard error of the mean (SEM). The statistical significance of differences between experimental conditions were assessed using either Student's t-test or analysis of variance (ANOVA) with Bonferroni correction using GraphPad Prism (version 8.0) analysis software. Differences in the mean of experimental conditions was considered significant if the probability value (p-value) was <0.05. All immunoblotting figures are representative.

Acknowledgments

We thank staff at the MRC PPU International Centre for Kinase Profiling (University of Dundee, UK) for providing us with the inhibitor panel used for screening. We thank E. Allen, J. Stark, and A. Muir for help and assistance with tissue culture, and the cloning, antibody and protein production teams within MRC PPU Reagents and Services (University of Dundee, UK), coordinated by J. Hastie and H. McLauchlan. We thank Dr. R. Clarke from the flow cytometry facility (School of Life Sciences, University of Dundee, UK) for her invaluable help and advice with Annexin V staining assays.

Funding

LDH is supported by the UK Medical Research Council (MRC) PhD studentship. NJD is supported by the UK MRC grant awarded to PC. GPS is supported by the U.K. MRC (Grant MC_UU_12016/3) and the pharmaceutical companies supporting the Division of Signal Transduction Therapy (Boehringer-Ingelheim, GlaxoSmithKline, Merck-Serono).

Competing Interests

The authors declare that they have no competing interests.

References

- 1 Siegel PM, Massagué J. Cytostatic and apoptotic actions of TGF- β in homeostasis and cancer. *Nat Rev Cancer* 2003; **3**: 807–820.
- 2 Xu J, Lamouille S, Derynck R. TGF- β -induced epithelial to mesenchymal transition. *Cell*

594 *Res* 2009; **19**: 156–172.

595 3 David CJ, Massagué J. Contextual determinants of TGF β action in development,
596 immunity and cancer. *Nat Rev Mol Cell Biol* 2018; **19**: 419–435.

597 4 Zhang Y, Alexander PB, Wang X-F. TGF- β Family Signaling in the Control of Cell
598 Proliferation and Survival. *Cold Spring Harb Perspect Biol* 2017; **9**: a022145.

599 5 Li MO, Flavell RA. TGF- β : A Master of All T Cell Trades. *Cell* 2008; **134**: 392–404.

600 6 Massagué J. TGF β signalling in context. *Nat Rev Mol Cell Biol* 2012; **13**: 616–630.

601 7 Massagué J. TGF β in Cancer. *Cell* 2008; **134**: 215–230.

602 8 Ikushima H, Miyazono K. TGF β signalling: a complex web in cancer progression. *Nat*
603 *Rev Cancer* 2010; **10**: 415–424.

604 9 Drabsch Y, ten Dijke P. TGF- β signalling and its role in cancer progression and
605 metastasis. *Cancer Metastasis Rev* 2012; **31**: 553–568.

606 10 Bierie B, Moses HL. TGF β : the molecular Jekyll and Hyde of cancer. *Nat Rev Cancer*
607 2006; **6**: 506–520.

608 11 Inman GJ. Switching TGF β from a tumor suppressor to a tumor promoter. *Curr Opin*
609 *Genet Dev* 2011; **21**: 93–99.

610 12 Akhurst RJ, Hata A. Targeting the TGF β signalling pathway in disease. *Nat Rev Drug*
611 *Discov* 2012; **11**: 790–811.

612 13 Akhurst RJ. Targeting TGF- β Signaling for Therapeutic Gain. *Cold Spring Harb Perspect*
613 *Biol* 2017; **9**: a022301.

614 14 Connolly EC, Freimuth J, Akhurst RJ. Complexities of TGF- β targeted cancer therapy.
615 *Int J Biol Sci* 2012; **8**: 964–78.

616 15 Wrana JL, Attisano L, Wieser R, Ventura F, Massagué J. Mechanism of activation of
617 the TGF- β receptor. *Nature* 1994; **370**: 341–347.

618 16 Zhang Y, Feng X-H, Wu R-Y, Derynck R. Receptor-associated Mad homologues
619 synergize as effectors of the TGF- β response. *Nature* 1996; **383**: 168–172.

620 17 Massagué J, Hata A. TGF- β signalling through the Smad pathway. *Trends Cell Biol*
621 1997; **7**: 187–192.

622 18 Massagué J, Seoane J, Wotton D. Smad transcription factors. *Genes Dev* 2005; **19**:
623 2783–810.

624 19 Shi Y, Massagué J. Mechanisms of TGF- β Signaling from Cell Membrane to the
625 Nucleus. *Cell* 2003; **113**: 685–700.

626 20 Hill CS. Transcriptional control by the SMADs. *Cold Spring Harb Perspect Biol* 2016; **8**:
627 a022079.

628 21 Rojas-Fernandez A, Herhaus L, Macartney T, Lachaud C, Hay RT, Sapkota GP. Rapid
629 generation of endogenously driven transcriptional reporters in cells through
630 CRISPR/Cas9. *Sci Rep* 2015; **5**: 9811.

631 22 Keeton MR, Curriden SA, van Zonneveld AJ, Loskutoff DJ. Identification of regulatory
632 sequences in the type 1 plasminogen activator inhibitor gene responsive to
633 transforming growth factor beta. *J Biol Chem* 1991; **266**: 23048–52.

634 23 Dennler S, Itoh S, Vivien D, ten Dijke P, Huet S, Gauthier JM. Direct binding of Smad3
635 and Smad4 to critical TGF beta-inducible elements in the promoter of human
636 plasminogen activator inhibitor-type 1 gene. *EMBO J* 1998; **17**: 3091–100.

637 24 Abe M, Harpel JG, Metz CN, Nunes I, Loskutoff DJ, Rifkin DB. An Assay for
638 Transforming Growth Factor- β Using Cells Transfected with a Plasminogen Activator
639 Inhibitor-1 Promoter-Luciferase Construct. *Anal Biochem* 1994; **216**: 276–284.

640 25 Bright NJ, Thornton C, Carling D. The regulation and function of mammalian AMPK-
641 related kinases. *Acta Physiol* 2009; **196**: 15–26.

642 26 Shackelford DB, Shaw RJ. The LKB1–AMPK pathway: metabolism and growth control
643 in tumour suppression. *Nat Rev Cancer* 2009; **9**: 563–575.

644 27 DaCosta Byfield S, Major C, Laping NJ, Roberts AB. SB-505124 is a selective inhibitor
645 of transforming growth factor-beta type I receptors ALK4, ALK5, and ALK7. *Mol*
646 *Pharmacol* 2004; **65**: 744–52.

647 28 Vogt J, Traynor R, Sapkota GP. The specificities of small molecule inhibitors of the
648 TGF β and BMP pathways. *Cell Signal* 2011; **23**: 1831–1842.

649 29 Tojo M, Hamashima Y, Hanyu A, Kajimoto T, Saitoh M, Miyazono K *et al.* The ALK-5
650 inhibitor A-83-01 inhibits Smad signaling and epithelial-to-mesenchymal transition by
651 transforming growth factor-beta. *Cancer Sci* 2005; **96**: 791–800.

652 30 Callahan JF, Burgess JL, Fornwald JA, Gaster LM, Harling JD, Harrington FP *et al.*
653 Identification of novel inhibitors of the transforming growth factor beta1 (TGF-beta1)
654 type 1 receptor (ALK5). *J Med Chem* 2002; **45**: 999–1001.

655 31 Rena G, Bain J, Elliott M, Cohen P. D4476, a cell-permeant inhibitor of CK1,
656 suppresses the site-specific phosphorylation and nuclear exclusion of FOXO1a. *EMBO*
657 *Rep* 2004; **5**: 60–5.

- 658 32 Cuny GD, Yu PB, Laha JK, Xing X, Liu J-F, Lai CS *et al.* Structure–activity relationship
659 study of bone morphogenetic protein (BMP) signaling inhibitors. *Bioorg Med Chem*
660 *Lett* 2008; **18**: 4388–4392.
- 661 33 Clark K, MacKenzie KF, Petkevicius K, Kristariyanto Y, Zhang J, Choi HG *et al.*
662 Phosphorylation of CRTC3 by the salt-inducible kinases controls the interconversion
663 of classically activated and regulatory macrophages. *Proc Natl Acad Sci U S A* 2012;
664 **109**: 16986–91.
- 665 34 Altarejos JY, Montminy M. CREB and the CRTC co-activators: sensors for hormonal
666 and metabolic signals. *Nat Rev Mol Cell Biol* 2011; **12**: 141–151.
- 667 35 Sonntag T, Moresco JJ, Vaughan JM, Matsumura S, Yates JR, Montminy M. Analysis of
668 a cAMP regulated coactivator family reveals an alternative phosphorylation motif for
669 AMPK family members. *PLoS One* 2017; **12**: e0173013.
- 670 36 Hawley SA, Boudeau J, Reid JL, Mustard KJ, Udd L, Mäkelä TP *et al.* Complexes
671 between the LKB1 tumor suppressor, STRAD α/β and MO25 α/β are upstream kinases
672 in the AMP-activated protein kinase cascade. *J Biol* 2003; **2**: 28.
- 673 37 Woods A, Johnstone SR, Dickerson K, Leiper FC, Fryer LGD, Neumann D *et al.* LKB1 Is
674 the Upstream Kinase in the AMP-Activated Protein Kinase Cascade. *Curr Biol* 2003;
675 **13**: 2004–2008.
- 676 38 Lizcano JM, Göransson O, Toth R, Deak M, Morrice NA, Boudeau J *et al.* LKB1 is a
677 master kinase that activates 13 kinases of the AMPK subfamily, including MARK/PAR-
678 1. *EMBO J* 2004; **23**: 833–43.
- 679 39 Darling NJ, Toth R, Simon J, Arthur C, Clark K. Inhibition of SIK2 and SIK3 during
680 differentiation enhances the anti-inflammatory phenotype of macrophages. 2017.
681 doi:10.1042/BCJ20160646.
- 682 40 Brown KA, Aakre ME, Gorska AE, Price JO, Eltom SE, Pietenpol JA *et al.* Induction by
683 transforming growth factor- β 1 of epithelial to mesenchymal transition is a rare event
684 in vitro. *Breast Cancer Res* 2004; **6**: R215.
- 685 41 Ozdamar B, Bose R, Barrios-Rodiles M, Wang H-R, Zhang Y, Wrana JL. Regulation of
686 the polarity protein Par6 by TGF β receptors controls epithelial cell plasticity.
687 *Science (80-)* 2005; **307**: 1603–9.
- 688 42 Ramjaun AR, Tomlinson S, Eddaoudi A, Downward J. Upregulation of two BH3-only
689 proteins, Bmf and Bim, during TGF β -induced apoptosis. *Oncogene* 2007; **26**: 970–981.

690 43 Avery-Cooper G, Doerr M, Gilbert RW, Youssef M, Richard A, Huether P *et al.* Par6 is
691 an essential mediator of apoptotic response to transforming growth factor beta in
692 NMuMG immortalized mammary cells. *Cancer Cell Int* 2014; **14**: 19.

693 44 Liu Y, He K, Hu Y, Guo X, Wang D, Shi W *et al.* YAP modulates TGF- β 1-induced
694 simultaneous apoptosis and EMT through upregulation of the EGF receptor. *Sci Rep*
695 2017; **7**: 45523.

696 45 Ozanne J, Prescott AR, Clark K. The clinically approved drugs dasatinib and bosutinib
697 induce anti-inflammatory macrophages by inhibiting the salt-inducible kinases.
698 *Biochem J* 2015; **465**: 271–9.

699 46 Sundberg TB, Choi HG, Song J-H, Russell CN, Hussain MM, Graham DB *et al.* Small-
700 molecule screening identifies inhibition of salt-inducible kinases as a therapeutic
701 strategy to enhance immunoregulatory functions of dendritic cells. *Proc Natl Acad Sci*
702 *U S A* 2014; **111**: 12468–73.

703 47 Keating GM. Dasatinib: A Review in Chronic Myeloid Leukaemia and Ph+ Acute
704 Lymphoblastic Leukaemia. *Drugs* 2017; **77**: 85–96.

705 48 Rosti G, Castagnetti F, Gugliotta G, Baccarani M. Tyrosine kinase inhibitors in chronic
706 myeloid leukaemia: which, when, for whom? *Nat Rev Clin Oncol* 2017; **14**: 141–154.

707 49 Datta PK, Blake MC, Moses HL. Regulation of plasminogen activator inhibitor-1
708 expression by transforming growth factor-beta -induced physical and functional
709 interactions between smads and Sp1. *J Biol Chem* 2000; **275**: 40014–9.

710 50 Binder BR, Christ G, Gruber F, Grubic N, Hufnagl P, Krebs M *et al.* Plasminogen
711 Activator Inhibitor 1: Physiological and Pathophysiological Roles. *Physiology* 2002; **17**:
712 56–61.

713 51 Kowanetz M, Lönn P, Vanlandewijck M, Kowanetz K, Heldin C-H, Moustakas A.
714 TGFbeta induces SIK to negatively regulate type I receptor kinase signaling. *J Cell Biol*
715 2008; **182**: 655–62.

716 52 Lönn P, Vanlandewijck M, Raja E, Kowanetz M, Watanabe Y, Kowanetz K *et al.*
717 Transcriptional induction of salt-inducible kinase 1 by transforming growth factor β
718 leads to negative regulation of type I receptor signaling in cooperation with the
719 Smurf2 ubiquitin ligase. *J Biol Chem* 2012; **287**: 12867–78.

720 53 Yang Y, Pan X, Lei W, Wang J, Song J. Transforming growth factor- β 1 induces
721 epithelial-to-mesenchymal transition and apoptosis via a cell cycle-dependent

722 mechanism. *Oncogene* 2006; **25**: 7235–7244.

723 54 Song J. EMT or apoptosis: a decision for TGF- β . *Cell Res* 2007; **17**: 289–290.

724 55 Inman GJ, Allday MJ. Apoptosis induced by TGF-beta 1 in Burkitt's lymphoma cells is
725 caspase 8 dependent but is death receptor independent. *J Immunol* 2000; **165**: 2500–
726 10.

727 56 Spender LC, O'Brien DI, Simpson D, Dutt D, Gregory CD, Allday MJ *et al*. TGF-beta
728 induces apoptosis in human B cells by transcriptional regulation of BIK and BCL-XL.
729 *Cell Death Differ* 2009; **16**: 593–602.

730 57 Spender LC, Carter MJ, O'Brien DI, Clark LJ, Yu J, Michalak EM *et al*. Transforming
731 growth factor- β directly induces p53-up-regulated modulator of apoptosis (PUMA)
732 during the rapid induction of apoptosis in myc-driven B-cell lymphomas. *J Biol Chem*
733 2013; **288**: 5198–209.

734 58 Kim B-C, Mamura M, Choi KS, Calabretta B, Kim S-J. Transforming growth factor beta
735 1 induces apoptosis through cleavage of BAD in a Smad3-dependent mechanism in
736 FaO hepatoma cells. *Mol Cell Biol* 2002; **22**: 1369–78.

737 59 Hsing AY, Kadomatsu K, Bonham MJ, Danielpour D. Regulation of apoptosis induced
738 by transforming growth factor-beta1 in nontumorigenic and tumorigenic prostatic
739 epithelial cell lines. *Cancer Res* 1996; **56**: 5146–9.

740 60 Edlund S, Bu S, Schuster N, Aspenström P, Heuchel R, Heldin N-E *et al*. Transforming
741 Growth Factor- β 1 (TGF- β)–induced Apoptosis of Prostate Cancer Cells Involves
742 Smad7-dependent Activation of p38 by TGF- β -activated Kinase 1 and Mitogen-
743 activated Protein Kinase Kinase 3. *Mol Biol Cell* 2003; **14**: 529–544.

744 61 Lin PH, Pan Z, Zheng L, Li N, Danielpour D, Ma JJ. Overexpression of Bax sensitizes
745 prostate cancer cells to TGF-beta induced apoptosis. *Cell Res* 2005; **15**: 160–166.

746 62 Strickson S, Emmerich CH, Goh ETH, Zhang J, Kelsall IR, Macartney T *et al*. Roles of the
747 TRAF6 and Pellino E3 ligases in MyD88 and RANKL signaling. *Proc Natl Acad Sci* 2017;
748 **114**: E3481–E3489.

749 63 Ran FA, Hsu PD, Wright J, Agarwala V, Scott DA, Zhang F. Genome engineering using
750 the CRISPR-Cas9 system. *Nat Protoc* 2013; **8**: 2281–2308.

751 64 Livak KJ, Schmittgen TD. Analysis of Relative Gene Expression Data Using Real-Time
752 Quantitative PCR and the 2- $\Delta\Delta$ CT Method. *Methods* 2001; **25**: 402–408.

753 65 Allan C, Burel J-M, Moore J, Blackburn C, Linkert M, Loynton S *et al*. OMERO: flexible,

754 model-driven data management for experimental biology. *Nat Methods* 2012; **9**:
755 245–253.
756

Figure Legends

Figure 1. Pharmacological screen in endogenous TGF β transcriptional reporter cells

A: Schematic representation of the dual-reporter cassette inserted in-frame with the ATG start codon of the endogenous *PAI-1* gene in U2OS human osteosarcoma cells.

B: Immunoblot analysis of wild type U2OS and U2OS 2G transcriptional reporter cell lines stimulated with TGF β_1 (5 ng mL⁻¹) for the indicated durations. Cell lysates were resolved via SDS-PAGE and membranes subjected to immunoblotting with the indicated antibodies.

C: Luciferase assay analysis of U2OS 2G transcriptional reporter cells incubated with either SB-505124 or DMSO control in the presence of TGF β_1 stimulation.

D: Immunoblot analysis of U2OS transcriptional reporter cells incubated with either SB-505124 or DMSO control in the presence of TGF β_1 stimulation. Cell lysates were resolved via SDS-PAGE and membranes subjected to immunoblotting with the indicated antibodies.

E: Schematic representation of the experimental workflow for the pharmacological screen in U2OS 2G transcriptional reporter cells.

F and G: The top 5 hits obtained from three independent experiments which reduced TGF β -induced luciferase activity. Data indicates the mean luciferase activity values (\pm SEM) relative to internal DMSO controls.

Figure 2. Characterisation of pharmacological SIK inhibitors in the context of TGF β signalling

A: The chemical structures of HG-9-91-01 and MRT199665, ATP-competitive small-molecule inhibitors of SIK isoforms.

B: Luciferase assay analysis of U2OS 2G transcriptional reporter cells incubated with either DMSO, SB-505124, HG-9-91-01 or MRT199665, in the presence or absence of TGF β_1 stimulation.

C: Immunoblot analysis of endogenous CRTC3 phosphorylation in wild type U2OS cells following incubation with DMSO, MRT199665 or HG-9-91-01. Cell lysates were subjected to endogenous CRTC3 immunoprecipitation (IP) and subsequently resolved via SDS-PAGE. Membranes were subjected to immunoblotting with the indicated antibodies.

D: Immunoblot analysis of wild type U2OS cells incubated with either SB-505124, HG-9-91-

01 or MRT199665 in the presence of TGF β ₁ stimulation. Cell lysates were resolved via SDS-PAGE and membranes subjected to immunoblotting with the indicated antibodies.

E: *In vitro* kinase assay analysis of recombinant constitutively active TGF β R1 (ALK5) in the presence of HG-9-91-01 or MRT199665 at the three indicated concentrations. Values denote the mean percentage activity remaining (\pm SD).

Figure 3. MRT199665 attenuates TGF β -mediated transcription in human cancer cell lines

A: Immunoblot analysis of U2OS 2G transcriptional reporter cells incubated with either SB-505124 or MRT199665 in the presence of TGF β ₁ stimulation. Cell lysates were resolved via SDS-PAGE and membranes subjected to immunoblotting with the indicated antibodies.

B: RT-qPCR analysis of *PAI-1* mRNA expression in wild type U2OS human osteosarcoma cells incubated with either SB-505124 or MRT199665 in the presence or absence of TGF β ₁ stimulation.

C: RT-qPCR analysis of *PAI-1*, *SMAD7* and *CTGF* mRNA expression in wild type A-172 human glioblastoma cells incubated with either SB-505124 or MRT199665 in the presence or absence of TGF β ₁ stimulation.

Figure 4. Genetic evidence for the involvement of SIK isoforms in TGF β -mediated PAI-1 expression

A: Sequence alignment of the activation segment of the human AMPK α catalytic subunits and the 13 members of the AMPK-related family of protein kinases. The asterisk indicates the conserved activation (T) loop threonine residue that is phosphorylated by LKB1.

B: RT-qPCR analysis of *PAI-1* mRNA expression in wild type HeLa cervical adenocarcinoma cells and HeLa cells overexpressing either LKB1^{WT} or LKB1^{D194A} following TGF β ₁ stimulation.

C: Immunoblot analysis of wild type HeLa cells and HeLa cells overexpressing either LKB1^{WT} or LKB1^{D194A} following TGF β ₁ stimulation. Cell lysates were resolved via SDS-PAGE and membranes subjected to immunoblotting with the indicated antibodies.

D: Immunoblot analysis of endogenous CRTC3 phosphorylation in wild type MEFs and MEFs derived from homozygous SIK2^{T175A}/SIK3^{T163A} KI mouse embryos. Cell lysates were subjected to endogenous CRTC3 IP and subsequently resolved via SDS-PAGE. Membranes were subjected to immunoblotting with the indicated antibodies.

63 **E:** Immunoblot analysis of wild type MEFs stimulated with TGF β ₁ for the indicated durations.
64 Cell lysates were resolved via SDS-PAGE and membranes subjected to immunoblotting with
65 the indicated antibodies.

66 **F:** Immunoblot analysis of wild type and homozygous SIK2^{T175A}/SIK3^{T163A} MEFs. Cell lysates
67 were resolved via SDS-PAGE and membranes subjected to immunoblotting with the
68 indicated antibodies.

69 **G:** RT-qPCR analysis of *PAI-1* mRNA expression in wild type and homozygous
70 SIK2^{T175A}/SIK3^{T163A} KI MEFs following TGF β ₁ stimulation.

71

72 **Figure 5. SIK inhibition enhances TGF β -independent cytostasis**

73 **A:** Immunoblot analysis of wild type HaCaT cells stimulated with TGF β ₁ for the indicated
74 durations. Cell lysates were resolved via SDS-PAGE and membranes subjected to
75 immunoblotting with the indicated antibodies.

76 **B:** Immunoblot analysis of wild type HaCaT cells incubated with either DMSO, SB-505124 or
77 MRT199665, in the presence or absence of TGF β ₁ stimulation. Cell lysates were resolved via
78 SDS-PAGE and membranes subjected to immunoblotting with the indicated antibodies.

79 **C:** Immunoblot analysis of wild type and homozygous SIK2^{T175A}/SIK3^{T163A} MEFs following
80 TGF β ₁ stimulation. Cell lysates were resolved via SDS-PAGE and membranes subjected to
81 immunoblotting with the indicated antibodies.

82 **D:** Immunoblot analysis of wild type and SMAD3^{-/-} HaCaT cells incubated in the presence or
83 absence of MRT199665. Cell lysates were resolved via SDS-PAGE and membranes subjected
84 to immunoblotting with the indicated antibodies.

85

86 **Figure 6. MRT199665 potentiates TGF β -mediated apoptotic cell death**

87 **A:** Immunoblot analysis of wild type NMuMG murine mammary epithelial cells stimulated
88 with TGF β ₁ for the indicated durations. Cell lysates were resolved via SDS-PAGE and
89 membranes subjected to immunoblotting with the indicated antibodies.

90 **B:** Immunoblot analysis of endogenous CRTC3 phosphorylation in wild type NMuMG cells
91 following incubation with DMSO, MRT199665 or HG-9-91-01. Cell lysates were subjected to
92 CRTC3 IP and subsequently resolved via SDS-PAGE. Membranes were subjected to
93 immunoblotting with the indicated antibodies.

94 **C:** Immunoblot analysis of wild type NMuMG cells incubated with either SB-505124 or
95 MRT199665 in the presence of TGF β_1 stimulation. Cell lysates were resolved via SDS-PAGE
96 and membranes subjected to immunoblotting with the indicated antibodies.

97 **D:** Immunoblot analysis of wild type NMuMG cells incubated with MRT199665 in the
98 presence or absence of TGF β_1 stimulation for the indicated durations. Cell lysates were
99 resolved via SDS-PAGE and membranes subjected to immunoblotting with the indicated
100 antibodies.

101 **E:** Annexin V staining analysis of wild type NMuMG cells incubated with DMSO, SB-505124
102 or MRT199665 in the presence of TGF β_1 stimulation. Data represents the percentage of cells
103 positive for annexin V staining from three independent experiments (5×10^4 cell counts per
104 sample per replicate).

105 **F:** Crystal violet cellular viability analysis of wild type NMuMG cells incubated with DMSO,
106 SB-505124 or MRT199665 in the presence of TGF β_1 stimulation. Data represents cellular
107 viability relative to unstimulated DMSO control cells.

108

109 **Figure 7. The clinically approved tyrosine kinase inhibitors (TKIs) bosutinib and dasatinib**
110 **impact TGF β -mediated transcriptional and cellular responses.**

111 **A:** The chemical structures of the clinically approved small-molecule tyrosine kinase
112 inhibitors (TKIs) bosutinib and dasatinib.

113 **B:** *In vitro* nanomolar IC₅₀ values of bosutinib and dasatinib against the protein kinases Abl,
114 BTK, Src and the three SIK isoforms (adapted from(Ozanne, Prescott and Clark, 2015)).

115 **C:** Immunoblot analysis of endogenous CRTC3 phosphorylation in wild type U2OS cells
116 following incubation with DMSO, MRT199665, bosutinib or dasatinib. Cell lysates were
117 subjected to CRTC3 IP and subsequently resolved via SDS-PAGE. Membranes were subjected
118 to immunoblotting with the indicated antibodies.

119 **D:** Immunoblot analysis of U2OS 2G transcriptional reporter cells incubated with either SB-
120 505124, bosutinib or dasatinib in the presence of TGF β_1 stimulation. Cell lysates were
121 resolved via SDS-PAGE and membranes subjected to immunoblotting with the indicated
122 antibodies.

123 **E:** Immunoblot analysis of wild type U2OS cells incubated with either SB-505124, bosutinib
124 or dasatinib in the presence of TGF β_1 stimulation. Cell lysates were resolved via SDS-PAGE

and membranes subjected to immunoblotting with the indicated antibodies.

F: Immunoblot analysis of wild type NMuMG cells incubated with SB-505124, MRT199665, bosutinib or dasatinib in the presence of TGF β_1 stimulation. Cell lysates were resolved via SDS-PAGE and membranes subjected to immunoblotting with the indicated antibodies.

G: Immunoblot analysis of wild type NMuMG cells incubated with SB-505124, MRT199665 or bosutinib in the presence of TGF β_1 stimulation. Cell lysates were resolved via SDS-PAGE and membranes subjected to immunoblotting with the indicated antibodies.

Figure 8. SIK2 and SIK3 isoforms phosphorylate SMAD3 *in vitro* however MRT199665 does not affect SMAD interaction or nuclear translocation

A: Sequence alignment of the eight human SMAD proteins. The asterisk indicates the amino acid residue in recombinant SMAD3 (Thr247) that was identified via phosphorylation-site mapping analysis.

B: Immunoblot analysis of wild type HaCaT cells and SMAD3^{-/-} cells following transient overexpression of either FLAG-SMAD3^{WT} or FLAG-SMAD3^{T247A} mutant, in the presence or absence of TGF β_1 stimulation. Cell lysates were resolved via SDS-PAGE and membranes subjected to immunoblotting with the indicated antibodies.

C: U2OS cells stably expressing GFP-SMAD4 were incubated with DMSO, SB-505124 or MRT199665 in the presence or absence of TGF β_1 stimulation. Cell lysates were subjected to GFP immunoprecipitation and resolved via SDS-PAGE. Membranes were subjected to immunoblotting with the indicated antibodies.

D: Immunoblot analysis of SMAD2 and SMAD3 localisation in wild type U2OS cells following incubation with either DMSO, SB-505124 or MRT199665, in the presence or absence of TGF β_1 stimulation. Cell lysates were separated into cytoplasmic (C) and nuclear (N) fractions, resolved via SDS-PAGE and membranes subjected to immunoblotting with the indicated antibodies.

E: Immunofluorescence analysis of U2OS cells stably expressing GFP-SMAD2 following incubation with DMSO, SB-505124 or MRT199665 in the presence or absence of TGF β_1 stimulation (images are representative). Scale bar indicates 10 μ m.

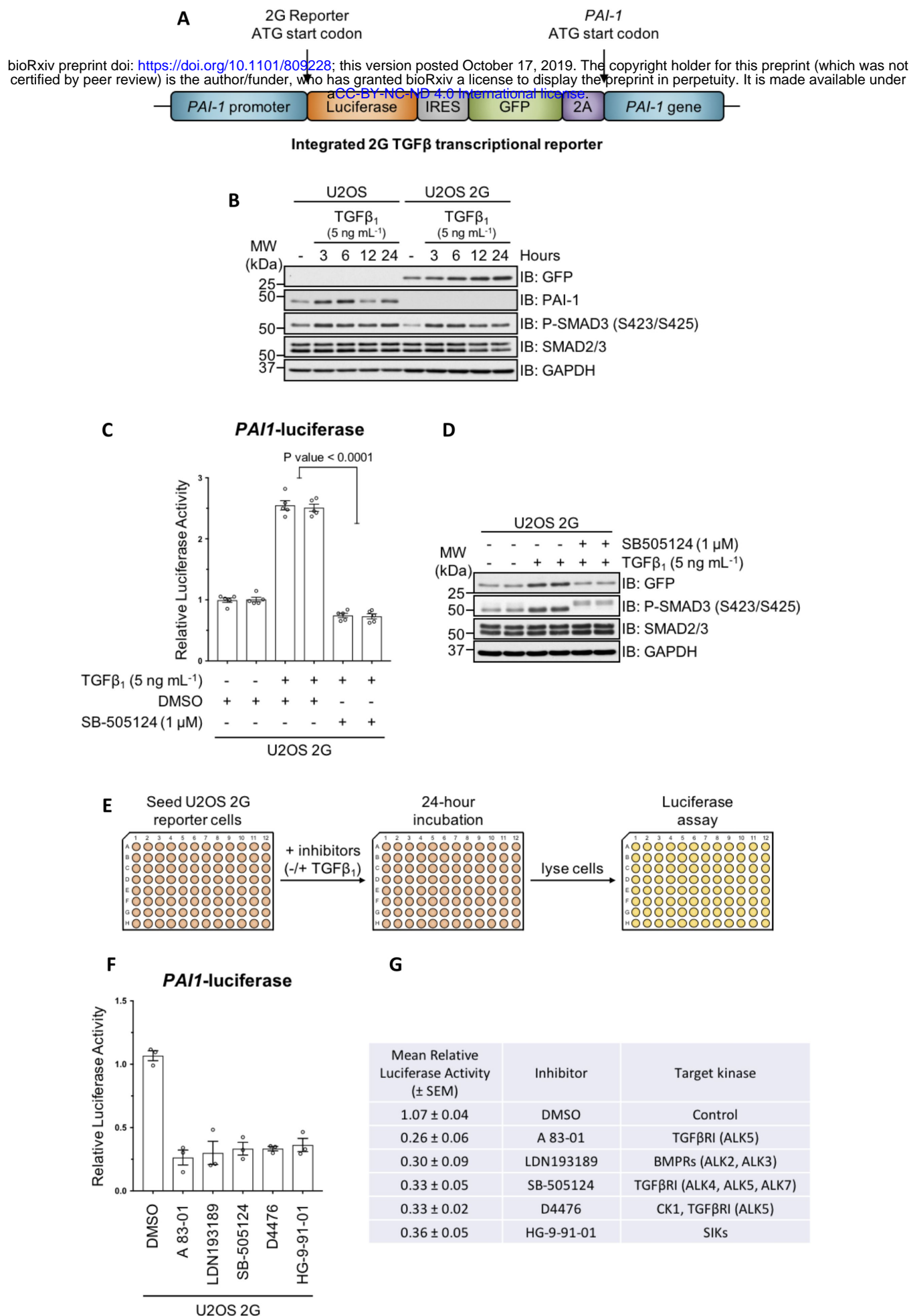


Figure 1.

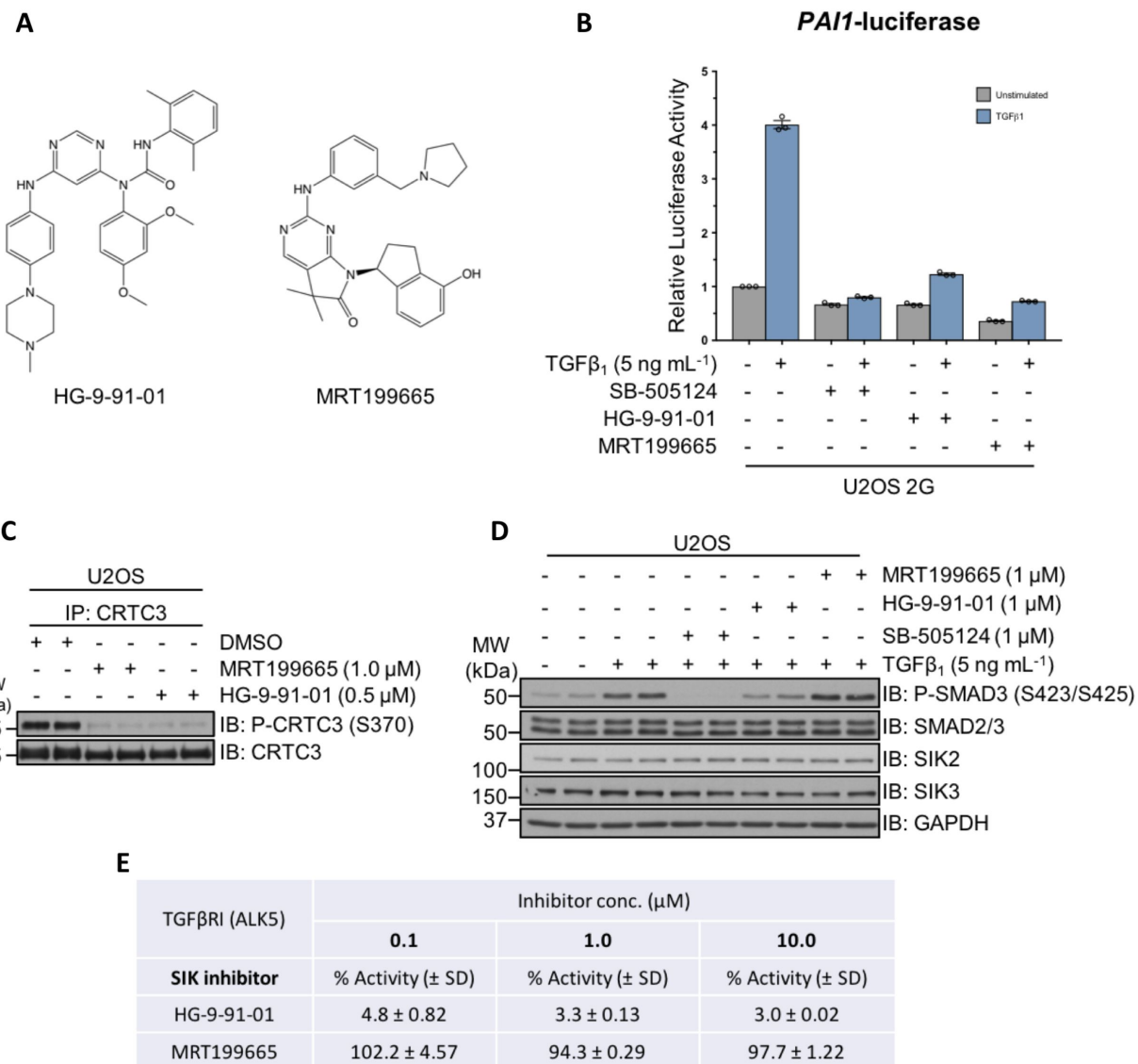


Figure 2.

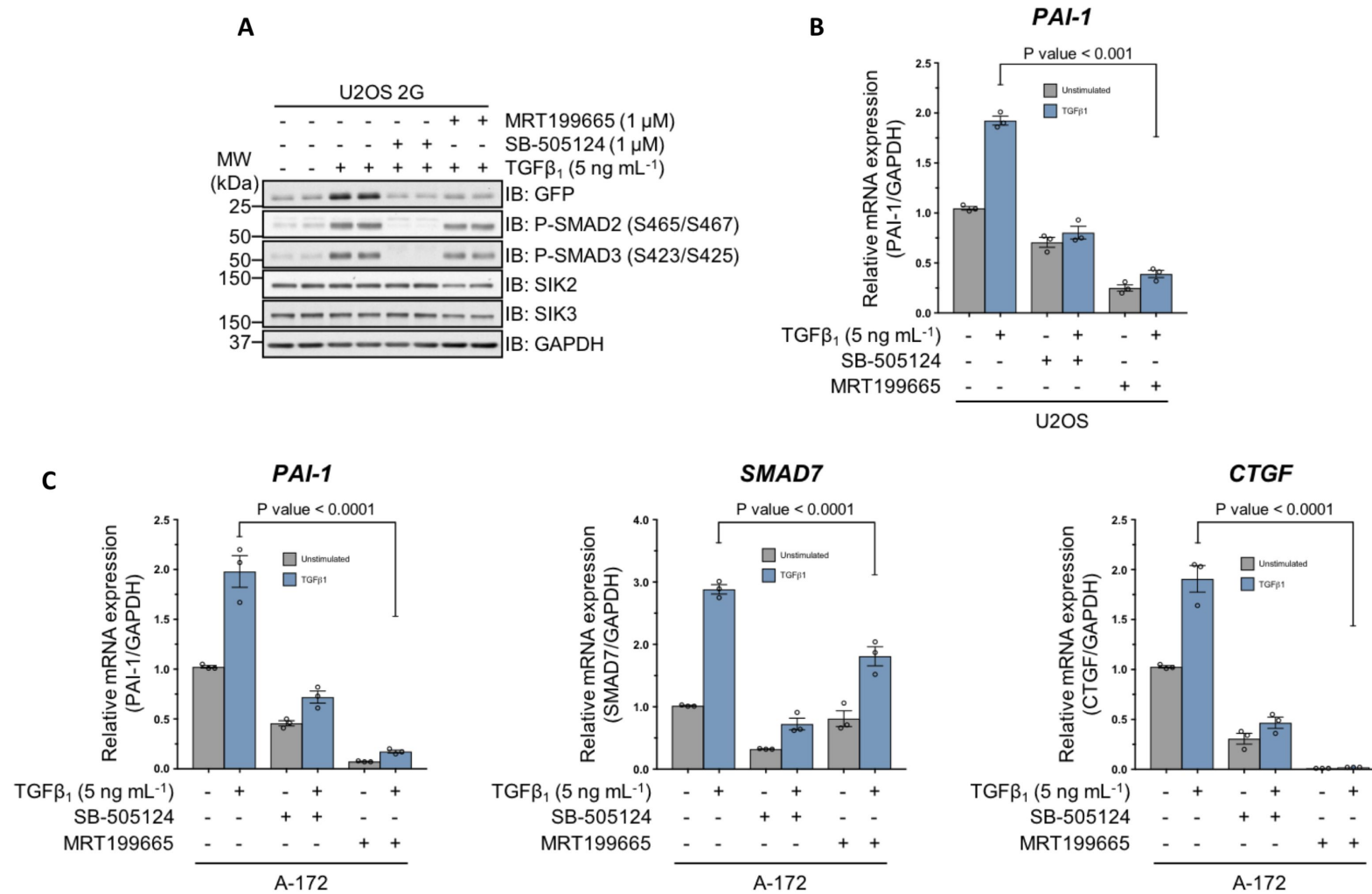


Figure 3.

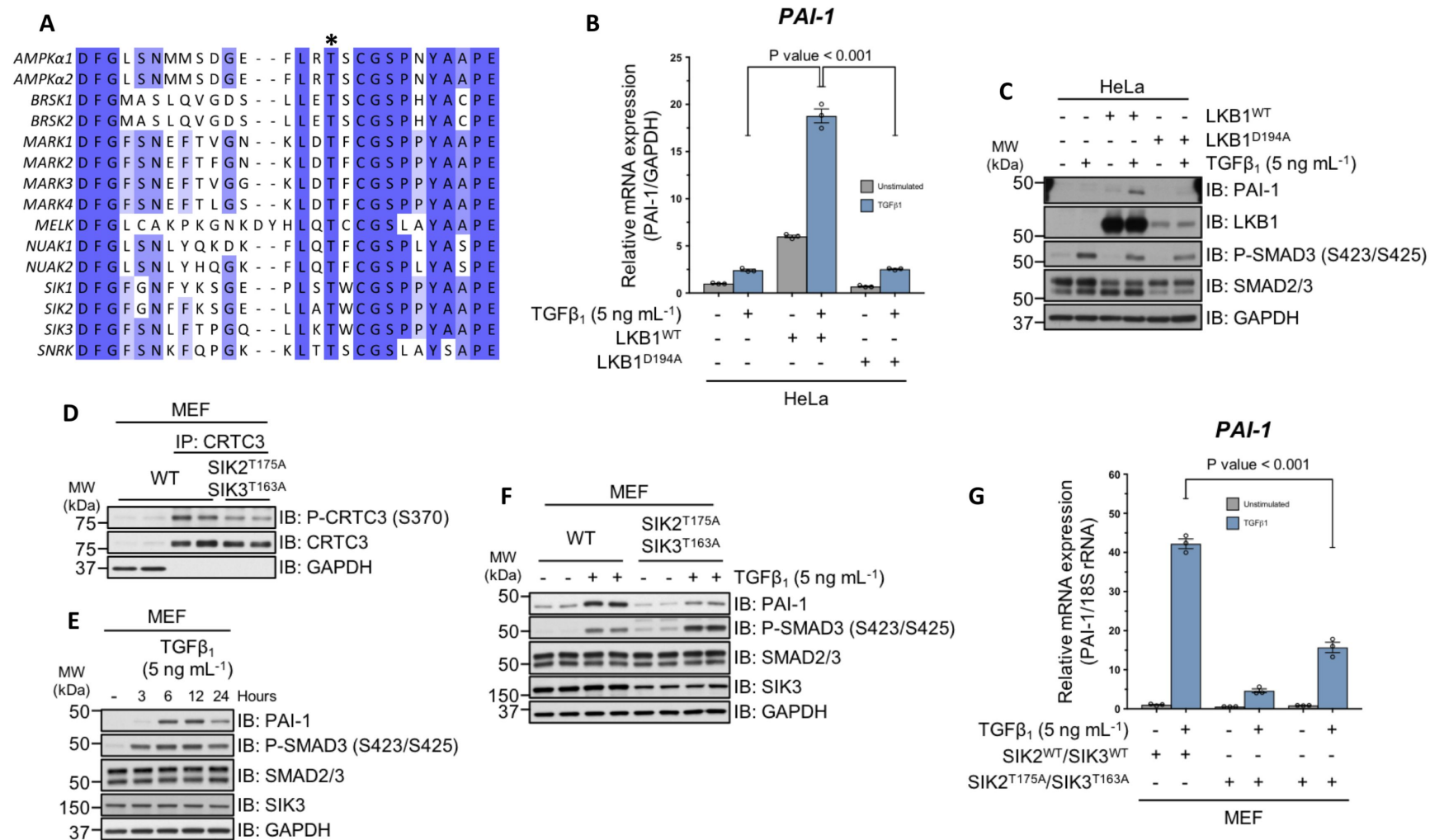


Figure 4.

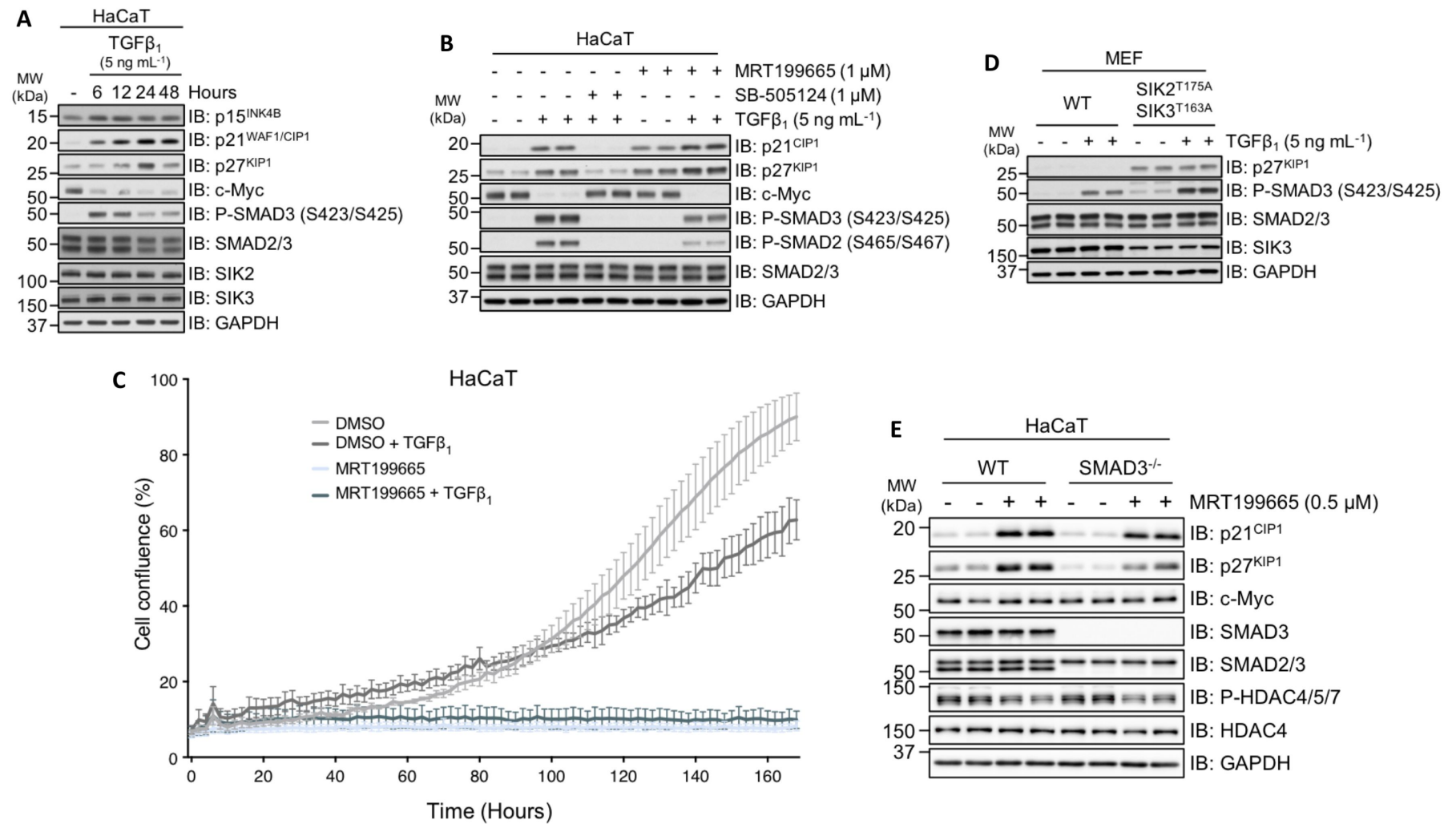


Figure 5.

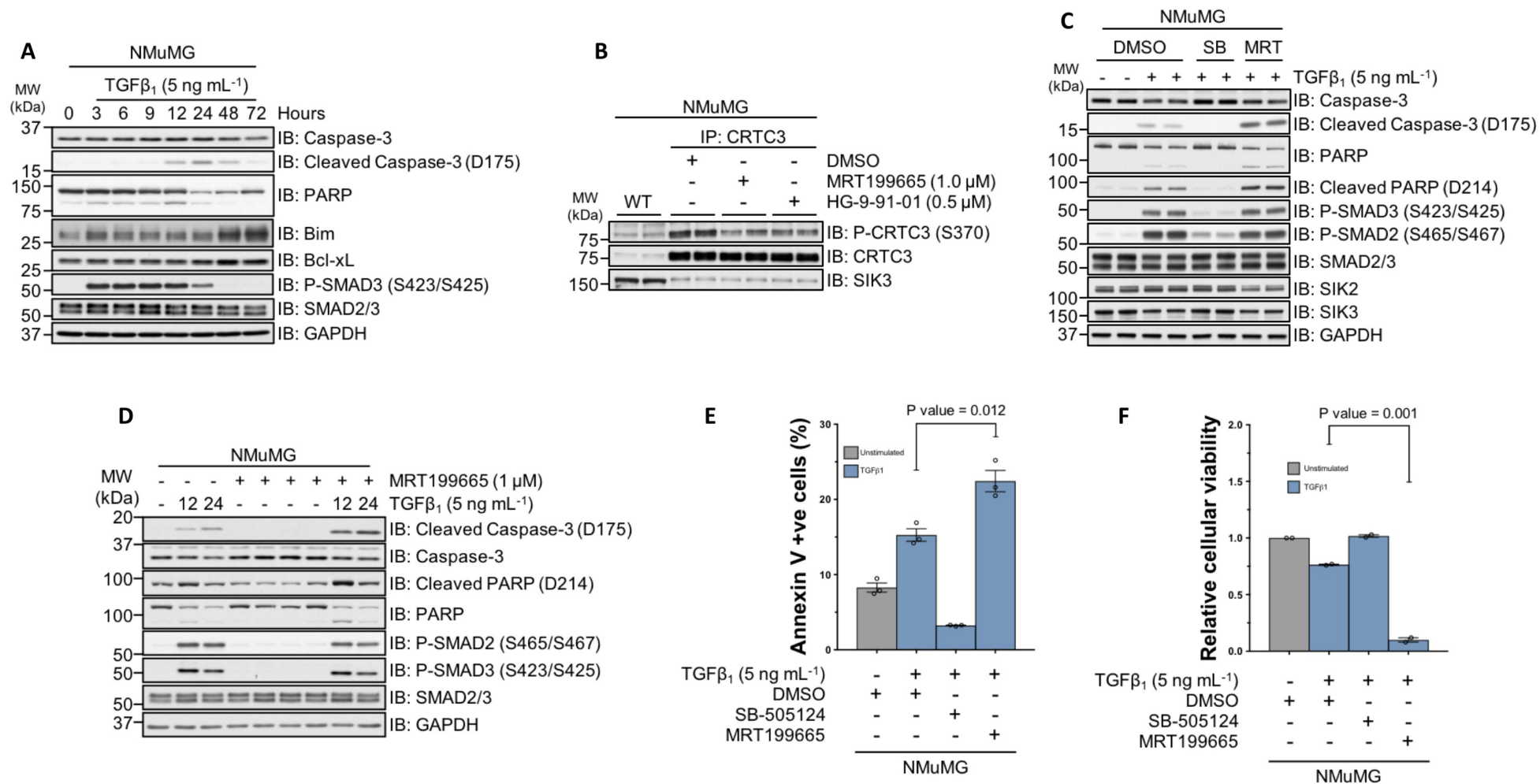


Figure 6.

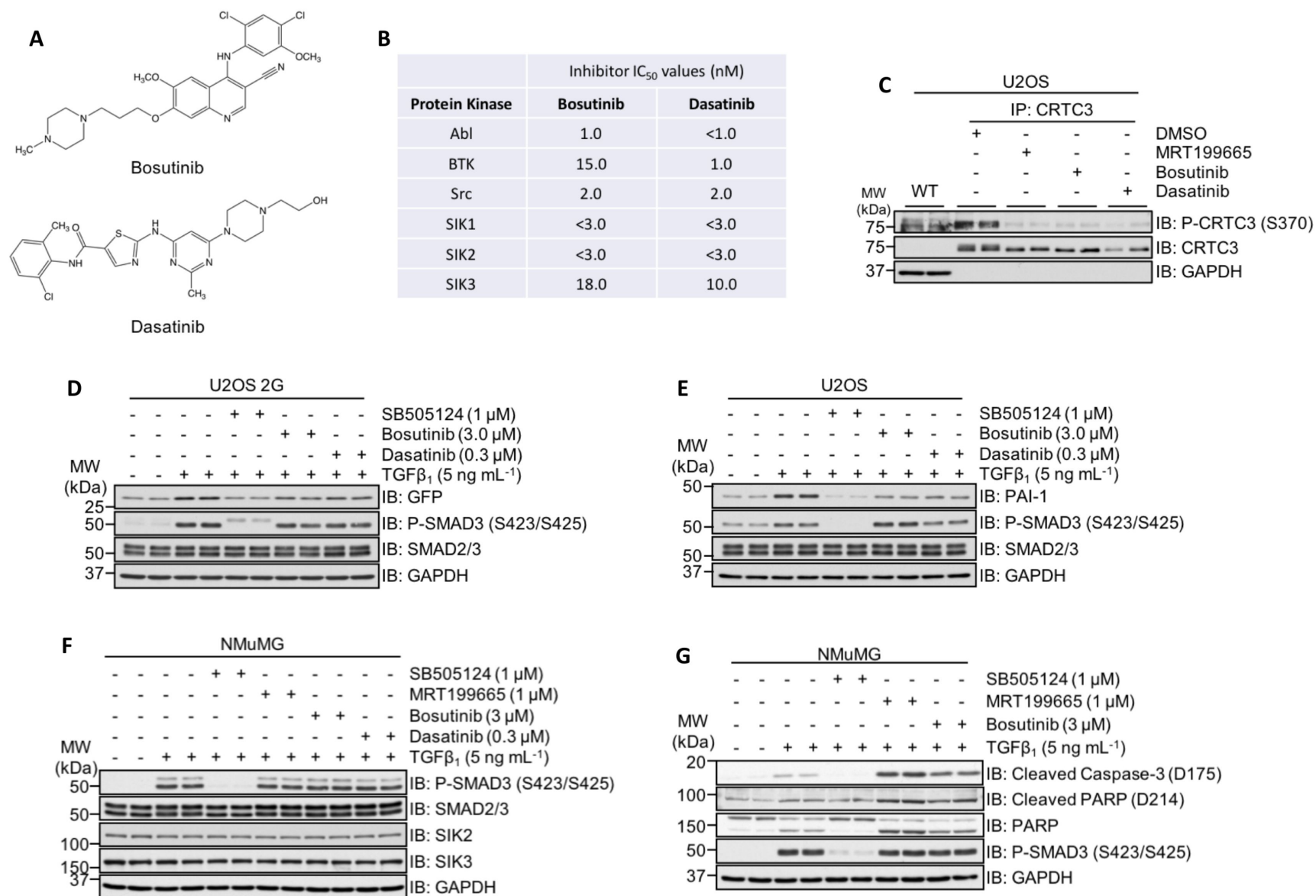


Figure 7.

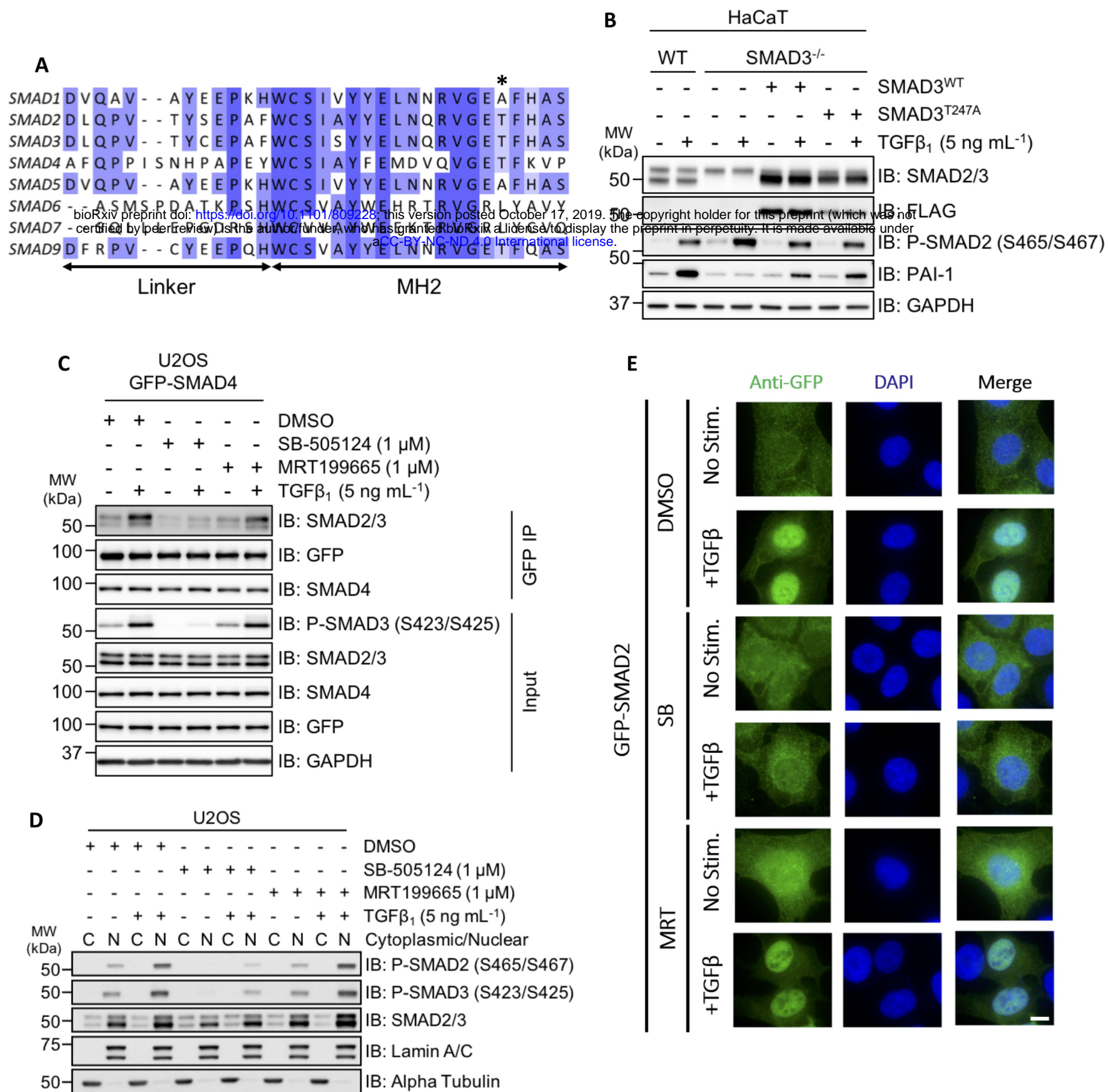


Figure 8.

Salt-inducible kinases (SIKs) regulate TGF β -mediated transcriptional and apoptotic responses

Luke D. Hutchinson¹, Nicola J. Darling¹, Stephanos Nicolaou^{2, #}, Ilaria Gori², Daniel R. Squair¹, Philip Cohen¹, Caroline S. Hill² and Gopal P. Sapkota^{1*}

Supplementary Figures and Legends:

Figure S1. *In vitro* phosphorylation of recombinant SMAD proteins

A: *In vitro* protein kinase assay analysis using the recombinant kinases MBP-SIK1, GST-SIK2 and GST-SIK3 and either recombinant SMAD2, SMAD3 or SMAD4 as the substrate. A constitutively active mutant form of the type I TGF β receptor (GST-TGF β RI^{T204D}) was included as a positive control.

Figure S2.

A: *In vitro* protein kinase assay analysis using the recombinant kinases GST-TGF β RI^{T204D}, GST-SIK2 and GST-SIK3 and cleaved recombinant SMAD3 as the substrate. The small-molecule inhibitors SB-505124 and HG-9-91-01 were included as controls.

B: Immunoblot analysis of wild type HaCaT cells and SMAD3^{-/-} cells following incubation with recombinant human TGF β ₁. Cell lysates were resolved via SDS-PAGE and membranes subjected to immunoblotting with the indicated antibodies.

C: Immunoblot analysis of wild type HaCaT cells and SMAD3^{-/-} cells following transient overexpression of either FLAG-SMAD3^{WT} or FLAG-SMAD3^{T247A} mutant, in the presence or absence of TGF β ₁ stimulation. Cell lysates were resolved via SDS-PAGE and membranes subjected to immunoblotting with the indicated antibodies.

